

Particle Temperature Measurements in a Flow Using Laser-Induced Phosphorescence

Kimberley C. Y. Kueh¹, Timothy C. W. Lau¹, Graham J. Nathan¹, Zeyad T. Alwahabi²

¹School of Mechanical Engineering, University of Adelaide
North Terrace, Adelaide, Australia
kimberley.kueh@adelaide.edu.au

²School of Chemical Engineering, University of Adelaide
North Terrace, Adelaide, Australia
zeyad.alwahabi@adelaide.edu.au

Abstract – the temperature of particles, heated by radiation, has been investigated using laser-induced phosphorescence. The particles were fluidised using an optically-accessible fluidised bed system, while the radiation was supplied by a solid state solar thermal simulator operated at ~915 nm. When the flux and the irradiation time was set at 19.7MW/m², the maximum particle's temperature and the average particle's temperature over 250s were 650 °C and 123 °C respectively.

Keywords: particles temperature, high solar flux, laser induced phosphorescence

1. Introduction

Many industrial and scientific applications rely on heat transfer within particle-laden flows. Therefore, it is important to develop techniques to enable a more comprehensive understanding of the parameters that control heat transfer in two-phase flows. In particular, the temperature change in moving particles subjected to radiative heating within a turbulent flow field has proven to be a key interest in the field as it not only will aid the development of the particle receiver technology, but also help in the improvement of process efficiencies of all applications utilising radiatively heated particles.

Over the past few decades, many studies have been performed to obtain a more comprehensive understanding of the gas-phase heat transfer in two-phase flows [1-5]. However, there are very little temperature measurement techniques that allows for the direct measurement of micro-meter particles in real time. This is because the in-situ measurement of moving particles is challenging and requires a technique that is highly sensitive. Recently, laser diagnostics have proven their potential to meet these criteria where they offers non-intrusive, spatially and temporally resolved measurements. In particular, laser-induced phosphorescence (LIP), which utilises temperature-dependent properties of thermophosphors offers the prospective of measuring particle temperatures directly. Previous studies from Abram et.al. [1] and Jovicic et.al. [6] have reported good accuracy while utilising the LIP technique, with errors as low as 5%.

Since the measurement of particles have a highly sensitive nature, a high flux, well-characterised heat source is desirable to minimise the unknown variables. That is, the heat source should provide enough heat such that the temperature of the particles would need to be significantly differentiable from the gas temperature during the short residence time particles within an unsteady two-phase flow would remain in the heating region. Lasers are known to be well-characterised and have the ability to provide high-flux radiation, as reported by Alwahabi et.al. [7]. The Solid-State Solar Thermal Simulator (SSSTS) generates the opportunity to establish a system that can provide in-situ measurements of temperature under conditions in which the heat transfer between the gas phase and particle phase is significant.

This paper aims to demonstrate the measurement of a non-intrusive, temporally resolved direct measurement of particles in an unsteady flow radiatively heated by well-characterised heat source. Additionally, it aims to demonstrate the role of attenuated heat in particle heat transfer.

2. Experiment

Three main sections comprised the experiment – a laser-induced phosphorescence (LIP) system for temperature measurement, a fluidised bed with optical access that generates unsteady flow of particles, and a controllable Solid-State Solar Thermal Simulator (SSSTS). A calibration experiment was also conducted prior to the experiment.

The particles were transported using an optically-accessible fluidised bed as shown in Figure 1. The fluidised bed has four circular apertures, aligned to allow the laser beam to pass through the axis of the reactor, and two measurement systems to be aligned perpendicular to the laser beams on either side of the reactor. To generate a uniform flow of fluidising gas, dry air supplied externally were channelled through two inlets and transported via layers of glass beads, followed by a sintered plate. In this case, dry air was used as the fluidising gas to avoid humidity and minimise agglomeration in the fluidised bed. A flow controller (Alicat Scientific, MC 20slpm) was used to maintain a constant airflow of 6.5 L/min. The outlet from the top of the fluidised bed was connected to an exhaust line to ensure stable air pressure and to remove any elutriated particles from the laboratory.



Fig. 1: Optically-accessible fluidized bed with four apertures – two to allow access for heating and excitation laser beams, and two for optical detection.

The Solid-State Solar Thermal Simulator (SSSTS) is a system that generates a focussed beam that converges to a waist of 10.5mm diameter and is capable of generating flux of up to 36.6MW/m^2 [7]. Importantly, the SSSTS waist spans a length of 20mm, the beam profile of which is constant throughout the waist length. This ensures an even heating region in the region of measurement in the fluidised bed. A K-type thermocouple is placed at the surface of its Fiber-optic Head (FOH) to monitor its temperature and ensure it does not exceed 50°C .

Fig. 2 shows the experimental setup of the present analysis. A third harmonic of the Nd:YAG (Quantel Q-smart 850) laser operated at $10.27 \pm 0.47\text{mJ}$ and 355nm was directed into a fluidised bed chamber to excite the TPs. Its laser beam path is offset from that of the SSSTS by 7° , the intercept of which was aligned such that it occurs at the centre of the fluidised bed. The phosphorescence emission signals emitted by excited particles were collected by a spectrometer via a two-lens light-collecting channel directed to a fibre bundle (Thorlabs, BFL200HS02). The resolved spectra were then recorded using an ICCD camera (Princeton Instruments-Max4). Additionally, a UV silica plate was placed 300mm away from the front of the FOH of the SSTS to split the irradiation beam into a 92:8 ratio. Both beams were then directed to water-cooled power meters (Gentec model HP100A-4KW-HE) that provided real-time power measurements at a sample frequency of 10HZ, as well as acted as beam dumps. Comparison of both power meter readings provide information about attenuation of heat flux by the particles, which indicates particle mass loading within the system.

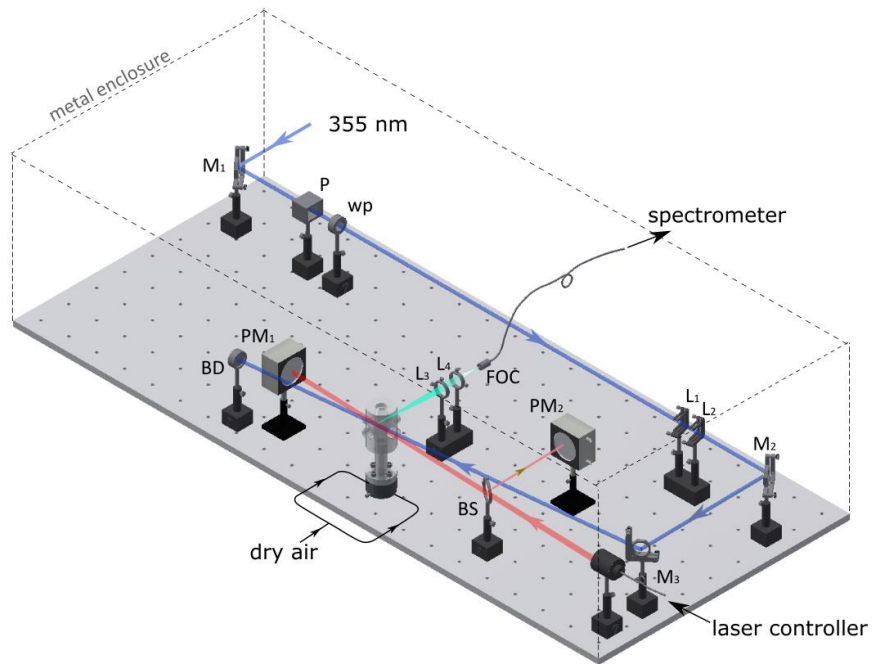


Fig. 2: Optical arrangement of experiment. Dark blue line: 355nm Nd:YAG laser beam path; Red line: 910nm SSSTS heating laser beam path; Light blue line: optical collection path of phosphorescence emission. M: Mirror, P: Polariser, wp: waveplate, L: lens, PM: power meter, BD: beam dump, BS: beam splitter, FOC: fibre-optic cable.

To relate the phosphorescence emission collected to temperature, a calibration experiment was done. The setup of temperature calibration experiment is similar to that described above, with the exception that instead of a fluidised bed, a plate coated with thermophosphors (TPs) and placed inside an oven (MTI Corporation, OTF-1200X-S) was used, as seen in Fig. 3. The temperature of the TP-coated plate was controlled electrically by an oven controller, as seen in Fig. 3. A K-type thermocouple was placed directly on the plate to measure the temperature of the plate in-situ.

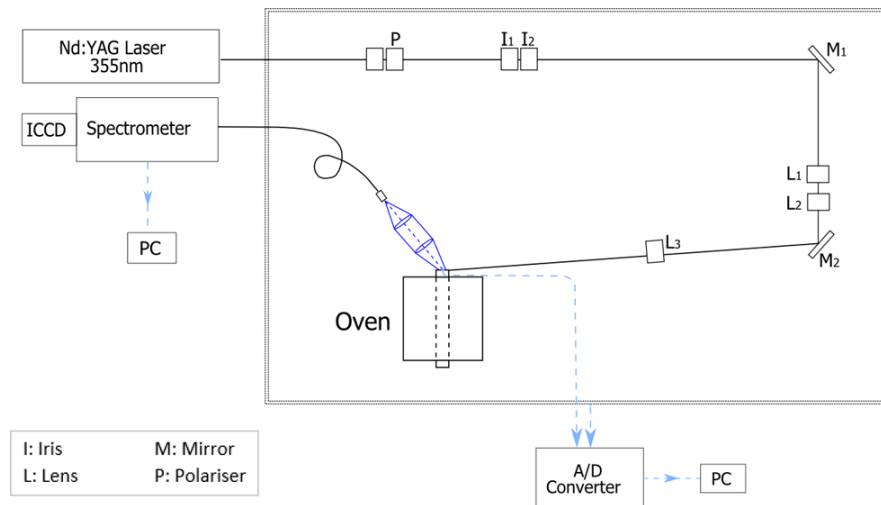


Fig. 3: Schematic of calibration setup of particle temperature. K-type thermocouples were attached on the thermophosphor-coated plated and safety box and were monitored at all times. P: polarizer, I: Iris, M: Mirror, L: Lens.

3. Results and Discussion

To select an appropriate TP for the current experiment, it is important to take into consideration the operating temperature and decaying lifetimes of the TPs as different TPs exhibits different properties based on these parameters. Thus, calculations based on a simple first-order heat transfer model was performed and parameters as closely matching the experiment as possible. It was found that the expected temperature range would be $< 627^{\circ}\text{C}$. Hence, the ZnO:Zn TP was selected due to its highly sensitive nature within this temperature range [8]. However, during initial investigations, it was found that ZnO:Zn TPs had a tendency to agglomerate. As such, the ZnO:Zn TPs were mixed together with $\text{CaSO}_4 \cdot 2\text{H}_2\text{O}$ particles with a volume ratio of 4:1 within the fluidised bed. The ZnO:Zn particles have a size distribution of $2\mu\text{m}$ - $50\mu\text{m}$, while the $\text{CaSO}_4 \cdot 2\text{H}_2\text{O}$ particles have a size distribution of $100\mu\text{m}$ - $200\mu\text{m}$. The larger $\text{CaSO}_4 \cdot 2\text{H}_2\text{O}$ particles promoted particle fluidisation by tending to break up any agglomerated particles of ZnO:Zn. However, only the ZnO:Zn TPs emit a phosphorescence signal when excited at the excitation wavelength of 355nm and exhibits thermo-phosphorescent properties which allows for temperature measurements.

3.1. Temperature Calibration

During the temperature calibration, 45 different temperatures were investigated ranging from 23°C to 423°C . At each temperature condition, the plate was allowed to reach thermal equilibrium, measured by the attached thermocouple, before the phosphorescence emissions were collected. The recorded spectra could then be visually compared, where a shift in the spectra with respect to wavelength is an indication of temperature sensitivity. Fig. 4 presents the normalised phosphorescence emission relative to wavelength at $T = 35^{\circ}\text{C}$, 103°C , 203°C and 300°C taken for the calibration experiment. It should be noted that although 45 different temperature conditions were investigated between 23°C and 425°C , only 4 are presented for clarity. A clear right shift in the peak wavelength position can be observed with increased temperature, demonstrating good sensitivity of ZnO:Zn to temperature throughout the recorded temperature range.

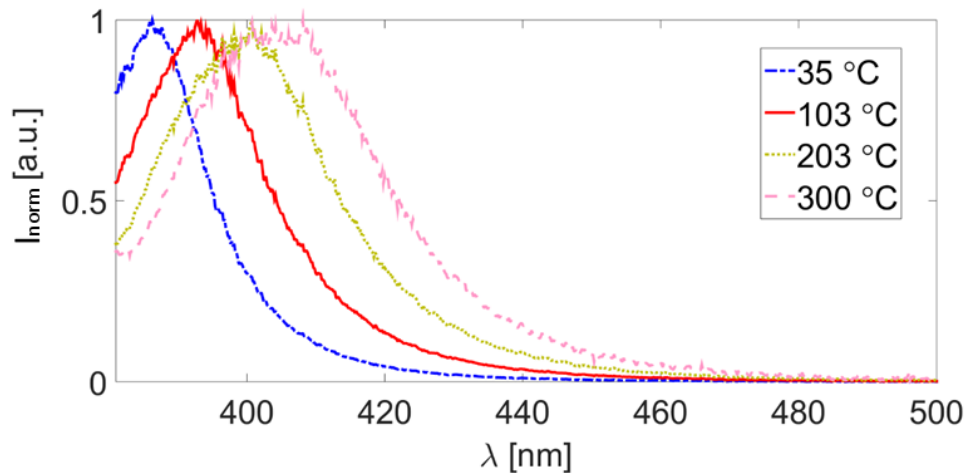


Fig. 4: Four normalised spectra emission as a function of wavelength, selected from a total of 45 cases for clarity.

To relate the measured phosphorescent emission intensity to temperature, intensity ratio, $\frac{I_{425}}{I_{390}}$ was used. In this case, $\frac{I_{425}}{I_{390}}$ was calculated with:

$$\frac{I_{425}}{I_{390}} = \frac{I_{410\text{nm}-440\text{nm}}}{I_{381\text{nm}-399\text{nm}}} \quad (1)$$

where the wavelength regions were chosen such that it would allow for a maximum sensitivity at the bandwidth of commercially-available filters for future experimental purposes. The resulting $\frac{I_{425}}{I_{390}}$ was then plotted against the temperature measured by the thermocouple as shown in Fig. 5: Calibration curve of ZnO:Zn temperature with respect to intensity ratio. The calibration curve for the remainder of the experiment. It was found that the relationship of the temperature and $\frac{I_{425}}{I_{390}}$ can be described with:

$$T\left(\frac{I_{425}}{I_{390}}\right) = -230.4\left(\frac{I_{425}}{I_{390}}\right)^2 + 500\frac{I_{425}}{I_{390}} + 23. \quad (2)$$

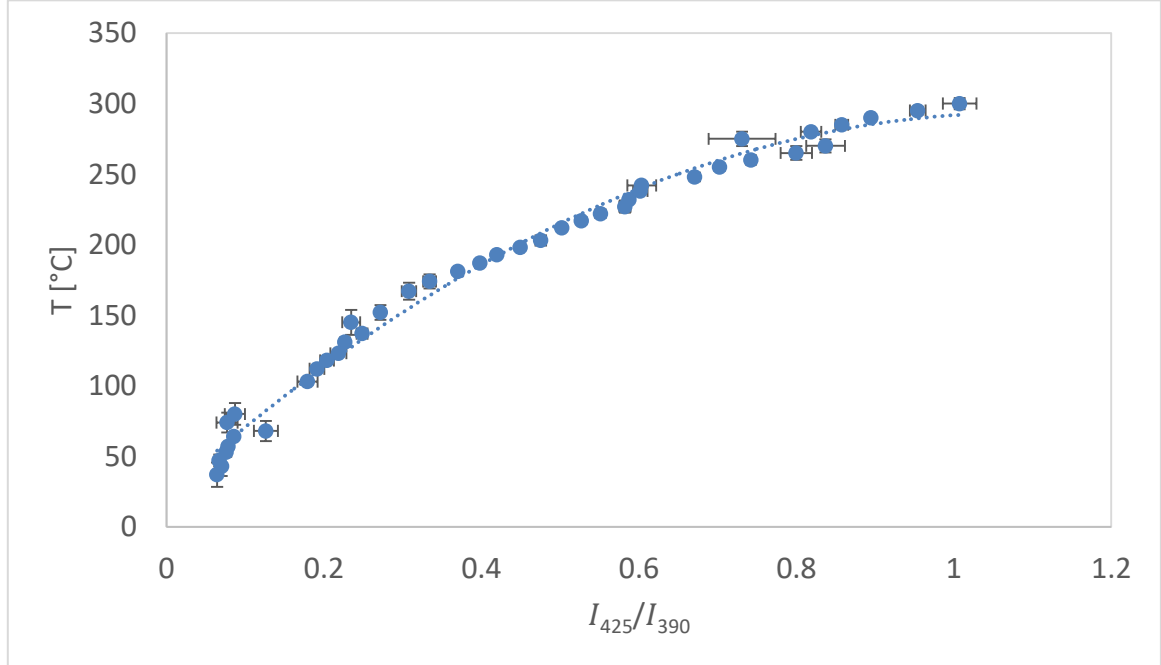


Fig. 5: Calibration curve of ZnO:Zn temperature with respect to intensity ratio.

3.2. Real Time Particle Temperature Measurement

To demonstrate the real time direct measurement of particle temperatures in turbulent flow, radiatively heated ZnO:Zn particles within a fluidised bed by the SSSTS were investigated. Here, the particles were heated at various irradiation fluxes, Φ , between 2.1MW/m^2 and 19.7MW/m^2 . 800 measurements over 340s were collected for each Φ , where the first 30s were of the particles at room temperature, followed by 250s of the SSSTS being switched on, and 60s of it being switched off. This is to aid in the investigation of the TP heat and cooling rates. After each measurement, and before the next, the particles in the fluidised bed were replenished and the system was allowed to cool to room temperature. Recorded phosphorescence emissions were then processed with in-house Matlab codes to infer $\frac{I_{425}}{I_{390}}$ and subsequently particle temperatures.

Fig. 6 presents the effect of Φ on (a) average particle temperature, $\Delta\bar{T}_p$, and (b) maximum particle temperature, $T_{p,max}$, for Φ between the range of 2.1MW/m^2 and 19.7MW/m^2 . Here, $\Delta\bar{T}_p$ is the average temperature of particles within the 250s that the SSSTS is switched on, while $T_{p,max}$ is the instantaneous maximum temperature measured. It was found that $\Delta\bar{T}_p$ and $T_{p,max}$ varied significantly from one another. For instance, when Φ was set to 19.7MW/m^2 , $\Delta\bar{T}_p$ was 123°C , while $T_{p,max}$ was measured at 650°C . An explanation for the large difference in $\Delta\bar{T}_p$ and $T_{p,max}$ is that particle mass loading within the fluidised bed plays a role in influencing particle temperatures (It should be noted that given the unsteady and turbulent nature of the fluidised bed, particle mass loading within the measurement section varies significantly from shot-to-shot). During the investigation, the TP temperatures were observed to rise almost instantaneously as the SSSTS was switched on, essentially demonstrating heating rates in the order of $23,000^\circ\text{C/s}$ at $\Phi = 21.1\text{MW/m}^2$.

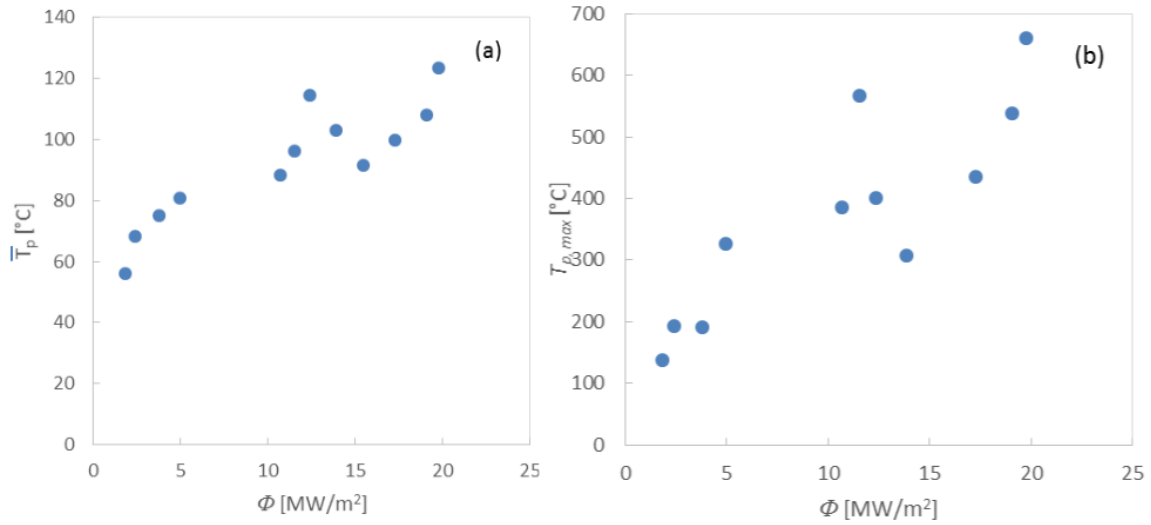


Fig. 6: Dependence of (a) average particle temperature, \bar{T}_p , and (b) maximum particle temperature, $T_{p,max}$, on irradiation flux, Φ .

Fig. 7 presents the T_p probability histogram of ZnO:Zn when it was heated at Φ (a) 1.85 MW/m², (b) 3.77 MW/m², (c) 7.83 MW/m², (d) 13.11 MW/m², (e) 13.86 MW/m², and (f) 15.44 MW/m². As it can be seen, as Φ was increased from 1.85 MW/m² to 13.11 MW/m², the probability of T_p reaching higher temperature increases consistently. However, the probability of T_p measured at high temperature is observed to decrease when Φ is further increased to 13.86 MW/m². This is consistent with the trends presented in Fig. 6 where a decreased $\Delta\bar{T}_p$ and $T_{p,max}$ were seen for Φ more than 13.11 MW/m². This indicates a dependence of T_p on particle mass loading in addition Φ . In order to better study the effects of heat transfer in particle-laden flow, a system that allows for good control of the particle mass loading, as well as well-defined flow field is needed for future investigations.

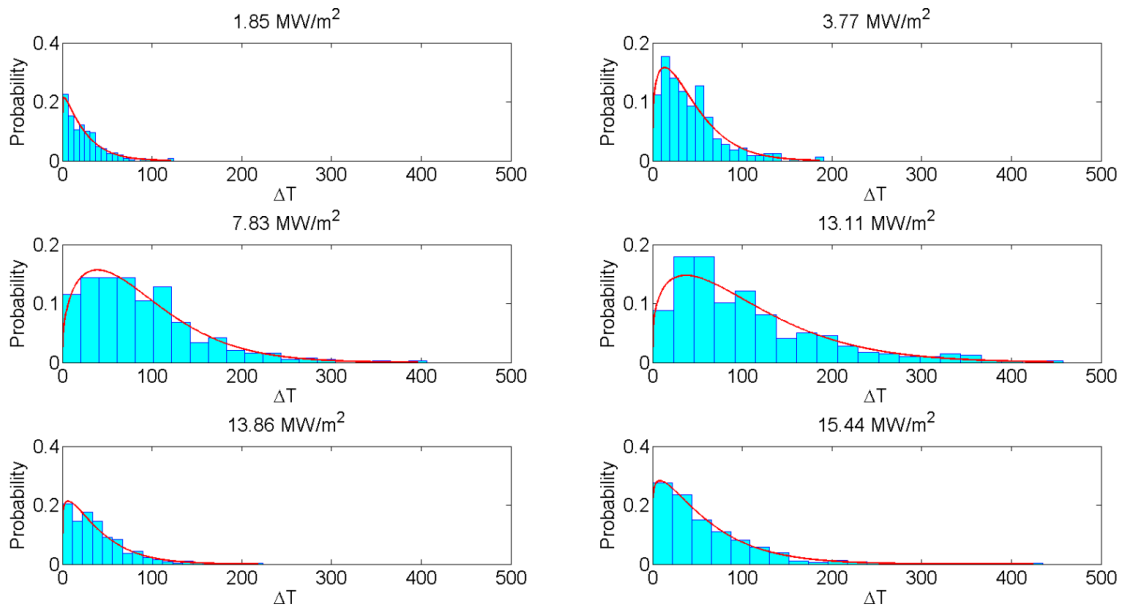


Fig. 7: Histogram of particle temperature probability at fluxes: (a) 1.85 MW/m², (b) 3.77 MW/m², (c) 7.83 MW/m², (d) 13.11 MW/m², (e) 13.86 MW/m², and (f) 15.44 MW/m².

4. Conclusion

Real-time direct measurement of ZnO:Zn particles temperatures has been demonstrated where particles in an optically-accessible fluidised bed were heated using a state-of-the-art solid-state solar thermal simulator (SSSTS) using laser-induced phosphorescence technique (LIP). This is done using a fibre-optical coupling to collect the phosphorescence. It was found that for the irradiation flux of 19.7MW/m^2 , a maximum particle temperature and average particle temperature measured in the unsteady fluid flow were $650\text{ }^\circ\text{C}$ and $123\text{ }^\circ\text{C}$ respectively. Particle mass loading, in addition to residence time and irradiation flux, were observed to play an important role in which particle temperature respond.

Acknowledgements

The financial support for the Australian Research Council is acknowledged (DP150102230). The authors would like to thank Mr Jeffrey Hiorns, form the mechanical workshop at the School of Chemical Engineering, for his outstanding technical support.

References

- [1] C. Abram, B. Fond, A. L. Heyes, F. Beyrau, "High-speed planar thermometry and velocimetry using thermographic phosphor particles," *Applied Physics B: Lasers and Optics*, vol. 111, pp. 155-160, 2013.
- [2] P. Basu, "Heat transfer in high temperature fast fluidized beds," *Chemical Engineering Science*, vol. 45, pp. 3123-3136, 1990.
- [3] H. Chen, Y. Chen, H.-T. Hsieh, N. Siegel, "Computational Fluid Dynamics Modeling of Gas-Particle Flow Within a Solid-Particle Solar Receiver," *Journal of Solar Energy Engineering*, vol. 129, pp. 160-170, 2006.
- [4] A. P. Collier, A. N. Hayhurst, J. L. Richardson, S. A. Scott, "The heat transfer coefficient between a particle and a bed (packed or fluidised) of much larger particles," *Chemical Engineering Science*, vol. 59, pp. 4613-4620, 2004.
- [5] M. S. Parmar, A. N. Hayhurst, "The heat transfer coefficient for a freely moving sphere in a bubbling fluidised bed," *Chemical Engineering Science*, vol. 57, pp. 3485-3494, 2002.
- [6] G. Jovicic, L. Zigan, S. Will, A. Leipertz, "Phosphor thermometry in turbulent hot gas flows applying Dy: YAG and Dy:Er:YAG particles," *Measurement Science and Technology*, vol. 26, 2015.
- [7] Z. T. Alwahabi, K. C. Y. Kueh, G. J. Nathan, S. Cannon, "Novel solid-state solar thermal simulator supplying 30,000 suns by a fibre optical probe," *Optics Express*, vol. 24, pp. A1444-A1453, 2016.
- [8] M. Aldén, A. Omrane, M. Richter, G. Sarner, "Thermographic phosphors for thermometry: A survey of combustion applications," *Progress in Energy and Combustion Science*, vol. 37, pp. 422-461, 2011.